Mechanical modelling of microwave sintering and experimental validation on an alumina powder

Maxence Renaux, Damien Méresse, Julien Pellé, Anthony Thuault, Céline Morin, Christelle Nivot, Christian Courtois

Mechanical modelling of microwave sintering and experimental validation on an alumina powder

Maxence Renaux[a,b,*], Damien Méresse[a,c], Julien Pellé[a], Anthony Thuault[b], Céline Morin[a,c], Christelle Nivot[b], Christian Courtois[b]

[a] *Univ. Polytechnique Hauts-de-France, LAMIH, CNRS, UMR 8201, F-59313 Valenciennes, France*
[b] *Univ. Polytechnique Hauts-de-France, LMCPA, EA 2443, F-59313 Valenciennes, France*
[c] *INSA Hauts-de-France, F-59313 Valenciennes, France*

Abstract

Microwave sintering (MW) allows fast heating ($\leq 30min$) and densification of ceramic materials, like alumina Al_2O_3. In order to predict the final material properties (density, size and grain size) the mechanical SOVS (Skorohold Olevsky Viscous Sintering) model is adapted and validated for conventional sintering of alumina. The model is implemented on ABAQUS with UMAT subroutine. Secondly, the SOVS model is modified for the microwave sintering by adapting the shear viscosity Arrhenius type law. Pre-exponential and exponential coefficients are modified for MW sintering. The calculated relative densities are compared to experimental results from conventional and microwave sintering and the relative difference remains under 3%. The coefficients identified for the MW sintering reveal a decrease in the shear viscosity by around 10 and an increase by up to 50 times in the grain boundaries diffusion coefficient.

Keywords: Mechanical SOVS model, Alumina, Sintering, Microwave, Densification

*Corresponding author
Email address: maxence.renaux@uphf.fr (Maxence Renaux)

Glossary

- ρ_D Density of fully dense material, kg.m^{-3}
- ρ_r Relative density
- $\rho_{r,0}$ Initial relative density
- d Grain size diameter, m
- d_0 Initial grain size diameter, m
- T Temperature, K
- ε_{ray} Emissivity of material
- σ Stress tensor, Pa
- ε Strain tensor
- $\dot{\varepsilon}$ Strain rate tensor, s^{-1}
- η Shear viscosity, Pa.s
- σ_s Sintering stress, Pa
- γ Surface energy, J.m^{-2}

- N_s Sintering exponant
- ξ Fit coefficient
- G_s Bulk viscosity modulus, Pa.s
- K_s Shear viscosity modulus, Pa.s
- ϕ Normalized bulk viscosity modulus
- ψ Normalized shear viscosity modulus

1. Introduction: Microwave sintering of ceramic

Studies on microwave sintering have been accelerated for less than twenty years. Indeed, this heating process has several advantages like reducing the time of heat treatment, improving the mechanical properties due to fine microstructures over conventional sintering, and many authors attempt to list the changes induced [1, 2]. Depending on the dielectric and magnetic properties of the considered material, it is possible to have a more uniform heating between the core and the skin of the material [1]. If a susceptor is used and due to the volumic heating, it is possible to obtain heating ramps up to several hundred degrees per minute, against a few tens for a conventional process. Orlik et al. [3] make a comparative study on BCTZ (Barium Titanate doped with Calcium and Zirconia) sintered by conventional (CS) and microwave (MW) heat treatments. Authors show that to obtain the same final relative density of 95% it is possible to reduce dwell time from 3 hours in CS to 1 hour in MW. Moreover, they shown that the MW sintering limited the grain size growth from $42.1\mu m$ (CS) to $24.1\mu m$ (MW). In the recent work of Curto et al. [4] on different grades of submicronic alumina like CT3000SG and P172LSB, a comparison between conventional and microwave heating is led at the sintering temperature of $1650°C$. To obtain the same range of final density between 93% and 97%, the dwell time is divided by 3 from 180 min to 60 min, the grain size decreases from (3.6 ± 0.8) μm to (2.4 ± 0.4) μm. This improves the mechanical properties: the elasticity modulus increases from 350 GPa to 370 GPa, the hardness is improved from 18 GPa to 21 GPa. So, modifications of sintering mechanisms due to electromagnetic field involved by microwave could modify the properties of sintered alumina.

In addition to the property modifications described above, some authors report a decrease in sintering temperature in microwave sintering. For example, Brosnan et al. [5] reports a 200°C decrease in sintering temperature for alumina in microwave sintering (2.45 GHz). Similar remarks have been made on other materials but the authors are cautious. Indeed, in a conventional furnace,

the temperature is measured using a thermocouple, whereas in microwave a contactless method like laser pyrometer is used. A measurement bias may exist between the two methods which could explain the potential decrease in sintering temperature. Many authors have tried to explain the differences in behaviour observed in microwave sintering, and the expression microwave effect is often used. There are thermal and athermal effects. For the first one, the high speed of microwave heating would generate thermal gradients on a microscopic scale [6, 7]. This would result in a local modification of the diffusion coefficients at the grain boundaries and in volume, thus increasing the concentrations of species or gaps. As a result, mass transport would be enhanced. Concerning the athermal effects, many authors study the influence of the electromagnetic field on the sintering, there would be an electromotive force. Rybakov et al. [8] report that there could be an intensification of the electric field at the grain boundary, leading to thermal runaway and increased species migration or transformation. The electric field would therefore be able to modify the sintering mechanisms (solid/solid, solid/gas) leading to a faster pores enclosure.

However, the causes of the changes in these mechanisms is not well understood. In order to optimize the microwave sintering, it is interesting to develop numerical modelling to predict the final properties of the material, to check its homogeneity and to optimize the process.

In this paper, a model with a mechanical approach will be used to model the evolution of the microstructural properties of a ceramic. It will be validated on the conventional sintering of alumina. Finally, the same model will be adapted to correlate the experimental results of microwave sintering.

2. Implementation of the SOVS model for the alumina

2.1. Densification modelling

In the litterature, there are several models for the alumina conventional sintering and for the microwave sintering. In both cases, two main approaches predominate: phenomenological models, based on experiments, and physical

models, based on fundamental approaches.

The phenomenological models consist in modeling the sintering by an Arrhenius type law as a function of parameters such as the temperature T, the grain size d and the relative density ρ_r from the initial relative density $\rho_{r,0}$. Several authors [9–11] propose a differential equation similar to the equation 1 where $f(\rho_r)$ and $g(d)$ are respectively functions dependent on density and grain size.

$$\frac{1}{\rho_r}\frac{d\rho_r}{dt} = K\frac{e^{-\frac{E_a}{RT}}}{T}\frac{f(\rho_r)}{g(d)} \tag{1}$$

The experimental measurements then consist in determining the f and g functions, the pre-exponential term K, and the activation energy E_a which depend on material parameters, the diffusion mechanisms and the process used. CHR (Constant Heating Rate) [9, 10, 12] and MSC (Master Sintering Curve) [2, 9] methods help to determine activation energies. For example, Zuo et al. [9] found a value of $E_a = 528kJ.mol^{-1}$ for the submicronic alumina with conventional sintering. This activation energy is only of $440kJ.mol^{-1}$ for the microwave sintering . It proves that microwave sintering affects the densification mechanisms. Bouvard et al. [11] proposed a densification law of Zirconia modeled by the equation 2. This densification law has been implemented on COMSOL Multiphysic in this work.

$$\frac{1}{\rho_r}\frac{d\rho_r}{dt} = \underbrace{200}_{K} e^{-\frac{20000}{T}} \underbrace{\left(\frac{1-\rho_r}{\rho_r-\rho_{r,0}}\right)^2}_{f(\rho_r)} \text{ with } \frac{E_a}{R} = 20000 \text{ and } g(d) = 1 \tag{2}$$

For physical models, a mechanical approach based on continuum mechanics is often preferred and coupled with a finite element software. Manière et al. [13] developped a model for the Zirconia microwave sintering based on the Olevsky model [14]. The behavior equation, in conventional and microwave sintering, is expressed in equation 3 and depends on the stress tensor σ_M and on the strain rate tensor $\dot{\varepsilon}_M$ (the subscript M corresponds to Manière equations):

$$\sigma_M = A_M\left[\varphi_M\dot{\varepsilon}_M + \left(\psi_M - \frac{1}{3}\varphi_M\right)tr(\dot{\varepsilon}_M)I\right] + \sigma_{s,M}I \tag{3}$$

Where φ and ψ are shear and bulk viscosity moduli, σ_s the sintering stress, A the shear viscosity according to Arrhenius law without grain size dependance,

I the identity matrix. All parameters will be more detailled in the next section. For the zirconia, the authors have shown from the experimental measurements and the simulations that the viscosity law A_M could be ajusted between CS and MW [13] and give values to A_0 and the equivalent activation energy Q and R the gas constant according to:

$$A_M = A_{0,M} T exp\left(\frac{Q}{RT}\right) \tag{4}$$

Compared to the conventional sintering, the shear viscosity in MW is adjusted by dividing by 2, and the results show that these modifications allow to model correctly the microwave sintering of the Zirconia. The lower value of the pre-exponential term $A_{0,M}$ allows to take into account the acceleration of the diffusive mass transport due to the high electric field gradient. This model might be adapted to alumina microwave sintering, but model parameters like viscosity correlation have to be determined. Other models seem to describe mechanical models for alumina conventional sintering. Van Nguyen et al. [15] describe three densification models for the conventional sintering of alumina, assisted or not by pressure: the Riedel model [16, 17], the Skorohold-Olevsky model [14, 18, 19] and the Abouaf model [20]. These three models are tested on an alumina cylindrical sample with a conventional pressure assisted sintering.

The models give good results with the experiments [15]. The modified Abouaf model minimizes the difference between experimental measurements and simulations, and seems to be the best to model the alumina densification. Nevertheless it requires determinating experimental parameters from mechanical and creep tests and calculating a large number of parameters. The modified SOVS (Shorohod Olevsky Viscous Sintering) model also allows to match between experimental measurements and simulated curves. A small gap is constated for the slope and the final value of the relative density. But this model is a compromise between the Abouaf model and the Riedel model which require to calculates more than 50 parameters or correlations. Moreover, Olevsky continues to work on the modelling of non-conventional sintering in particular for field-assisted sintering method like Spark Plasma Sintering (SPS) and microwave sintering

[14]. This could allow the model to evolve with the latest work.

In this work, the modified SOVS model is applied to the microwave sintering of the alumina. According to the litterature [15], this physical model has been retained because several studies of the litterature compares numerical simulations with experimental data on the conventional sintering of the alumina. Compared to the other physical based models, the lower number of parameters confirms this choice. Moreover, in the model, a viscosity law is used and take into account the influence of grain size coarsening. It seems important to take the grain size into account in the viscosity law. Indeed, this impacts the diffusion paths, the solid/solid and solid/gas interfaces. This differs slightly from Manière work with Zirconia (cf. equation 4). The modified SOVS model is implemented on a FEM (Finite Element Method) software (ABAQUS) using a user subroutine of material (UMAT) and is then validated with conventional sintering experiments. This step is required to check the validity of the law with our alumina powder, slightly different in its composition. The SOVS model is then used to simulate the microwave sintering of the alumina. A new set of parameters is identified to correlate with the relative density and the grain size obtained in microwave sintering experiments. The values of the identified parameters are finally discussed.

2.2. Details on the material constitutive equations

The SOVS model [19] is applied to alumina for conventional sintering [15, 21]. The model, initially developed by Skorohold, was modified by Olevsky and is based on continuum mechanics and Newtonian viscosity. The porous system consists of a skeleton with the constituent material and with pores homogeneously distributed. The system is assumed to be isotropic. The viscous behavior equation is nonlinear and consists of two parts: the first with a piston behavior law and the second taking into account the capillary forces which are applied and causes the closing of the porosities (sintering). This is expressed

by:

$$\sigma = \underbrace{2\eta\left[\varphi\dot{\varepsilon} + \psi Tr(\dot{\varepsilon})I\right]}_{\text{viscous part}} + \underbrace{\sigma_s I}_{\text{sintering stress part}} \tag{5}$$

Where σ is the Cauchy stress tensor, $\dot{\varepsilon}$ the deviatoric strain rate tensor, $Tr(\dot{\varepsilon})$ the trace of the strain rate tensor corresponding to the volume reduction, φ and ψ are normalized shear and bulk viscosity, η the shear viscosity of the fully dense core material. The densification rate $\frac{d\rho_r}{dt}$ is governed by the principle of mass conservation during sintering, and linked to the volume reduction $Tr(\dot{\varepsilon})$ and the relative density ρ_r by:

$$\frac{d\rho_r}{dt} = -\rho_r Tr(\dot{\varepsilon}) \tag{6}$$

The SOVS model is a physic-based model where only few parameters could be determined experimentally like the grain size and the shear viscosity, and expressed by a curve fitting. The authors [22, 23] suggest that the shear viscosity η should be expressed by an Arrhenius type law and takes into account of the grain growth. Moreover, Shinagawa compared and proposed expressions for the viscosity moduli φ and ψ [23] and the sintering stress σ_s [24] from experimental measurements. The sintering stress (eq. 7) represents a driving force for the sintering, and depends on the relative density ρ_r, the initial relative density $\rho_{r,0}$, the grain size d and the specific surface energy γ, with N_s and ξ fitting parameters:

$$\sigma_s = \frac{2\gamma}{\xi\frac{d}{2}}\rho^{N_s}\left[\frac{\rho_r(1-\rho_{r0})}{\rho_{r0}(1-\rho_r)}\right]^{\frac{1}{3}} \tag{7}$$

According to Shinagawa [24], the shear viscosity η is an Arrhenius law function of the temperature T and grain size d and expressed by the equation 8 from experimental measurements [24]. In the chosen temperature range the grain size d is supposed to be constant.

$$\eta = C_1 T exp(\frac{C_2}{T})d^3 \tag{8}$$

The evolution of grain size of pure alumina is given by the equation 9 [24] and depends on the temperature, the initial grain size d_0, a constant m and a grain

growth factor β:

$$d^m = d_0^m + \beta T \tag{9}$$

This equation would show that the grain size does not depend on time. However, in the case of sintering with a dwell time, the grain size would continue to increase with time. Futhermore,the grain size would start to grow at room temperature. Equation 9 should therefore be modified to take into account the evolution of microstructural properties with time and temperature. Moverover, it is reported in the litterature [2, 25] that the MgO doping inside alumina submicronic powder limits the grain size growth. A new grain growth law must be defined for conventional and microwave sintering. Authors, like Zuo et al. [2], propose, for MgO doped submicronic alumina sintered by conventional and microwave heating, a law where grain size is plotted versus the relative density. It looks to be applicable whatever sintering process, heating or dwell time, temperature treatments. The constitutive equation 5 is adapted as indicated in the equation 10 and takes into account of the temperature, the grain size and the relative density :

$$\sigma = 2G_s\dot{\varepsilon} + \left(K_s - \frac{2}{3}G_s\right) Tr(\dot{\varepsilon})I + \sigma_s I \tag{10}$$

The expressions of the viscosity moduli result from comparative studies [19, 23]. The effective shear viscosity G_s and the bulk viscosity K_s used in the equation 5 are defined by the equations 11 and 12 where n is an exponential constant.

$$G_s = \eta\varphi = \eta\rho_r^{2n-1} \tag{11}$$

$$K_s = 2\eta\psi = 3\left(\frac{1}{2.5\sqrt{1-\rho_r}}\right)^2 \eta\rho^{2n-1} \tag{12}$$

All the parameters and the constants used to simulate the conventional sintering of alumina are given in the Table 1 extracted from the Ref [15] and [23].

Parameters	Symbol	Value
Material constants for viscosity	C_1 $[Pa.s.K^{-1}.m^{-3}]$	7.82×10^{17}
	C_2 $[K]$	3.23×10^4
Exponential constant for viscosity	n	2.5
Exponential constant for sintering stress	N_s	5.0
Correction factor for sintering stress	ξ	0.5
Specific surface energy	γ $[J.m^{-2}]$	0.9
Exponent for grain evolution	m	1/0.37
Coefficient of grain size evolution	β $[m^{\frac{1}{0.37}}.K^{-1}]$	4.84×10^{-20}

Table 1: SOVS model parameters for pure alumina [15, 23]

2.3. Implementation on ABAQUS with UMAT subroutine

ABAQUS is used for the simulations with the modified SOVS model for alumina sintering. This is a commercially finite element based software. Nevertheless, the material behaviour law in Eq.5 is not a standard law. A user subroutine material (UMAT) is scripted in FORTRAN. The simulation process and the link between ABAQUS and the UMAT subroutine are described in Figure 1. First, the input parameters (geometry, temperature profile, initial density) are defined in ABAQUS. Then the UMAT subroutine imports data from ABAQUS at the previous increment time. The relative density is calculated according to the current position of the nodes. The variables, like shear viscosity and bulk viscosity, are updated according to the time step, the temperature field, the grain size and the previous material density. Thanks to this new set of parameters, a new stress tensor is calculated according to the equation 10. Finally, the stress tensor is exported to ABAQUS where a strain rate tensor, a strain tensor and a volume reduction are calculated for the given time step. This operation is repeated until the end of the sintering time simulated. The tensor equation could have been coded by another digital tool. However, ABAQUS was chosen in view of the possibility of coupling with a thermal model which could highlight thermal gradients depending on the configuration.

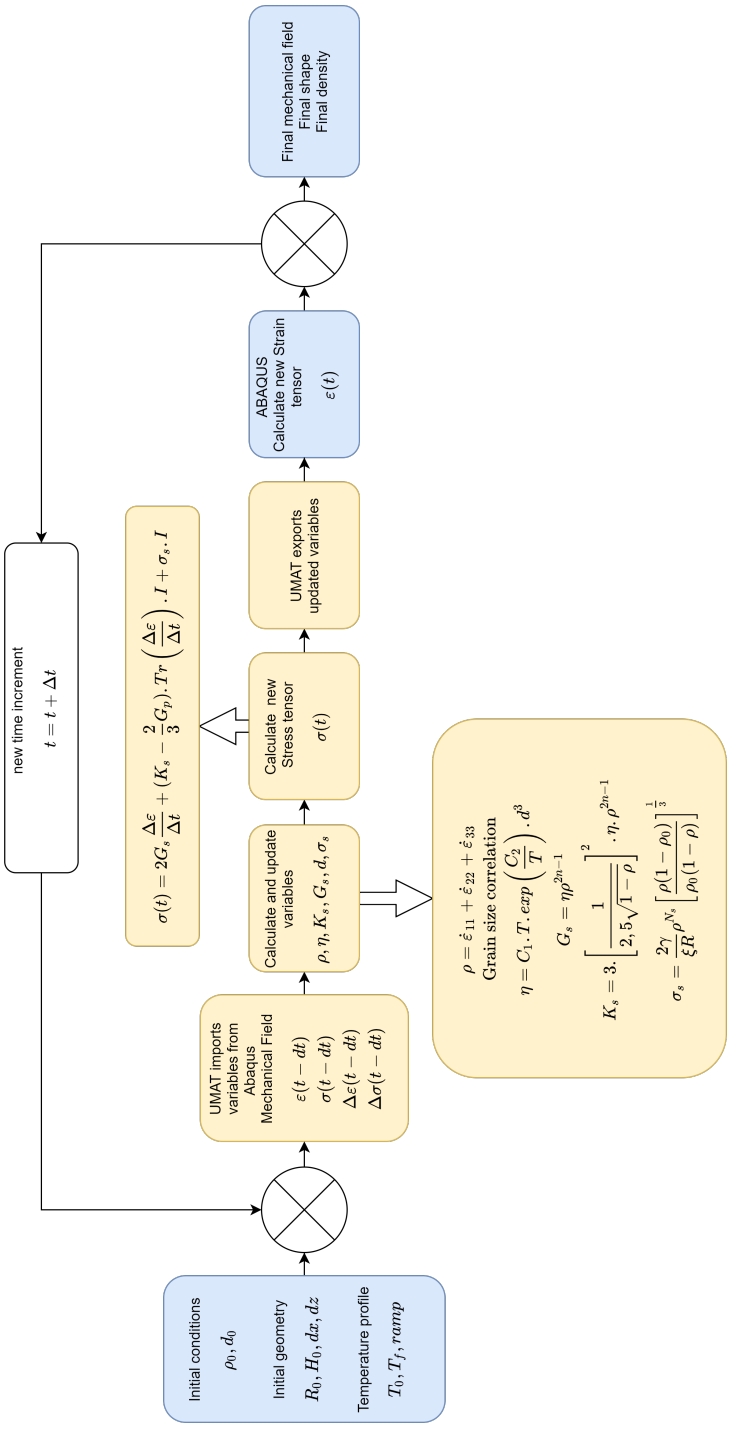

Figure 1: Calculation process for SOVS model on ABAQUS with UMAT subroutine

3. Validation of modified SOVS model on alumina conventional sintering

3.1. Material and experimental conditions

The material used for the experimental measurements is a CT3000SG alumina from Alcoa. The powder is slightly doped with MgO (0.07 %) with a grain size around $(0.25 \pm 0.01)\ \mu m$ ($D_{50} = 0.3\ \mu m$) obtained by laser granulometry and a specific surface area of $5.55\ g.cm^{-2}$. The powder is shaped by a uniaxial pressing, under a pressure of 2 tons. The pellet formed has a diameter of $13mm$ and a height of $10\ mm$. The mass of powder is $m = 3.00\ g$. The initial relative density measured by a geometrical method is (58 ± 1) %. For the conventional sintering, the samples are placed in a Thermoconcept oven (HTK 40 17 1750°C) and heated according to a ramp and then removed as soon as the temperature is reached. The density of the sintered sample is measured by Archimedes method in water. The range of the measured density spreads from 58% to 98% ±1%. The samples are then sliced and polished. A thermal etching is performed ($T_{etching} = T_{sintering} - 50°C$) in order to reveal the grain boundaries. Finally the samples are observed with a Scanning Electron Microscope (Jeol-JCM-6000) to measure the grain size which is calculated by the line intercept method [26].

3.2. Results and comparison with experimental measurements for conventional sintering

Due to the global cylindrical symmetry, the alumina sample is simplified in the model by a 2D axisymetric system. The material is supposed to be isotropic. Simulations are done with the previous alumina parameters (cf. Table 1), for a cylindrical sample (13 mm of diameter, 10 mm of height), initial density $\rho_{r,0} = 0.58$, initial grain size $d_0 = 250\ nm$, from 20°C to 1650°C according to ramps of $5°C/min$ and $10°C/min$. The temperature is supposed to be homogeneous inside the sample, and the temperature increase is imposed by ABAQUS

according to a given ramp. The relative density versus temperature curve is compared to the experimental results with the conventional sintering.

The figure 2 shows the comparison between modelling and experimental results for two heating rates, without (Eq 9) and with (Eq 13) gain size law modifications. First results (curve "SOVS CS 5°C/min, grain size Eq.9") without grain size adaption, show that the gap between model and experiments is higher than 50 %. In order to understand this difference investigation are led to the grain size and the necessity to adapt the equation 9.

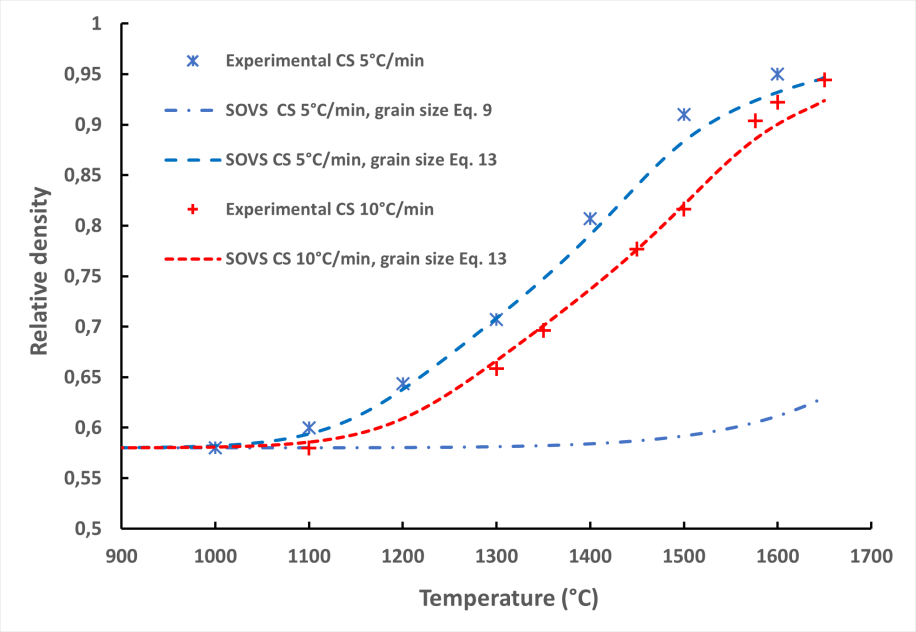

Figure 2: Comparison between experimental measurements and simulations for conventional sintering on alumina with two ramps of temperature

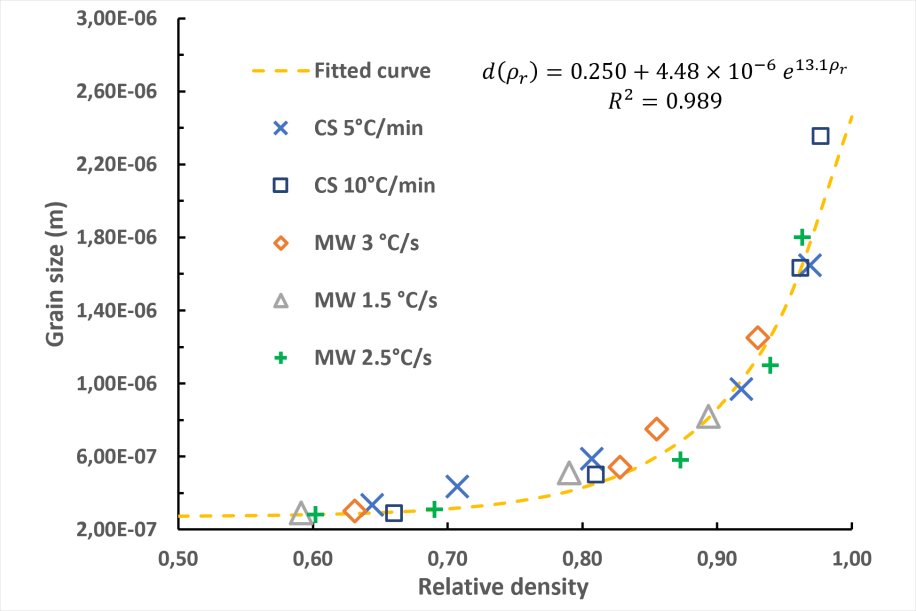

Figure 3: Grain size versus relative density, experimental results for different temperatures ramps, for CS and MW sintering

In the SOVS model, the grain size evolution law in Eq 9 is replaced by an experimental law. This modification allows to take into account MgO doping of CT3000SG alumina. A general fit can be deduced from our experimental results in Figure 3. An exponential curve fitted law ($R^2 = 0.989$) gives the diameter (in μm) from the density ($0.56 \leq \rho_r \leq 1$):

$$d(\rho_r) = 0.250 + 4.48 \times 10^{-6}.e^{13.1\rho_r} \text{ (with } d \text{ in } \mu m) \tag{13}$$

Simulations are performed to validate the SOVS model on conventional sintering tests with the grain size law adapted to the CT3000SG powder. Two heating ramps have been reproduced experimentally: 5°C/min and 10°C/min. The samples are pulled out of the oven as soon as the set temperature is reached. No holding time in the oven is applied. Then, each experimental point on the figure 2 represents a sintered sample. The results of the simulations for the two

heating ramps are also plotted. The average mean gap is 1%, and the maximum gap is around 2%. Slight gap of 2% is observed at the end of the sintering.

The conclusions of the simulation are, firstly, that it is possible to model the densification for MgO doped alumina. Secondly, it is important to take into account the grain size growth. To the overview of changing material, the grain size and the relative density could be accurately measured after sintering.

The modified SOVS model is then applied to a microwave sintering and the values of the viscous parameters are investigated to take into account the differences in the sintering mechanisms. All parameters are kept from initial SOVS model (Table 1), only the grain size law is adapted from the equation 13.

4. Application to microwave sintering of alumina

4.1. Microwave Sintering methods

In order to compare simulations to experimental measurements, alumina cylinders are sintered by microwave. The experimental set-up is presented in Figure 4. The microwave (cf. Figure 4 a) used is a microwave from the SAIREM company with a $2kW$ generator (GMP 20 KSM), with a working frequency of 2.45 GHz and a single mode resonant rectangular cavity (WR340, $a = 86.36mm$ and $b = 43.18mm$) working in TE_{105} mode, ie only the electric field can interact with the sample. The emissivity of the monochromatic pyrometer (Ircon, Modline 5, 350 to 2000 °C) used to measure the temperature is fixed at 0.8 for alumina [27]. As stated in the introduction, caution should be exercised when interpreting temperature readings with a pyrometer. A bias could exist between a value given by a thermocouple (in CS) and by the pyrometer (in MW). The sample is placed in a thermal insulating box of fibrous alumina / silica (Fiberfrax Duraboard) and surrounded by a silicon carbide (SiC) ring used as susceptor (cf. Figure 4 b). Everything is placed in the microwave cavity (cf. Figure 4 c). Samples are heated according to a specified ramp to a temperature range between $1000°C$ and $1650°C$. Once temperature is reached, the heating is switched off, and due to the fast cooling, the material properties are consid-

ered constant. As conventional sintering, final relative density are measured by Archimedes method in water.

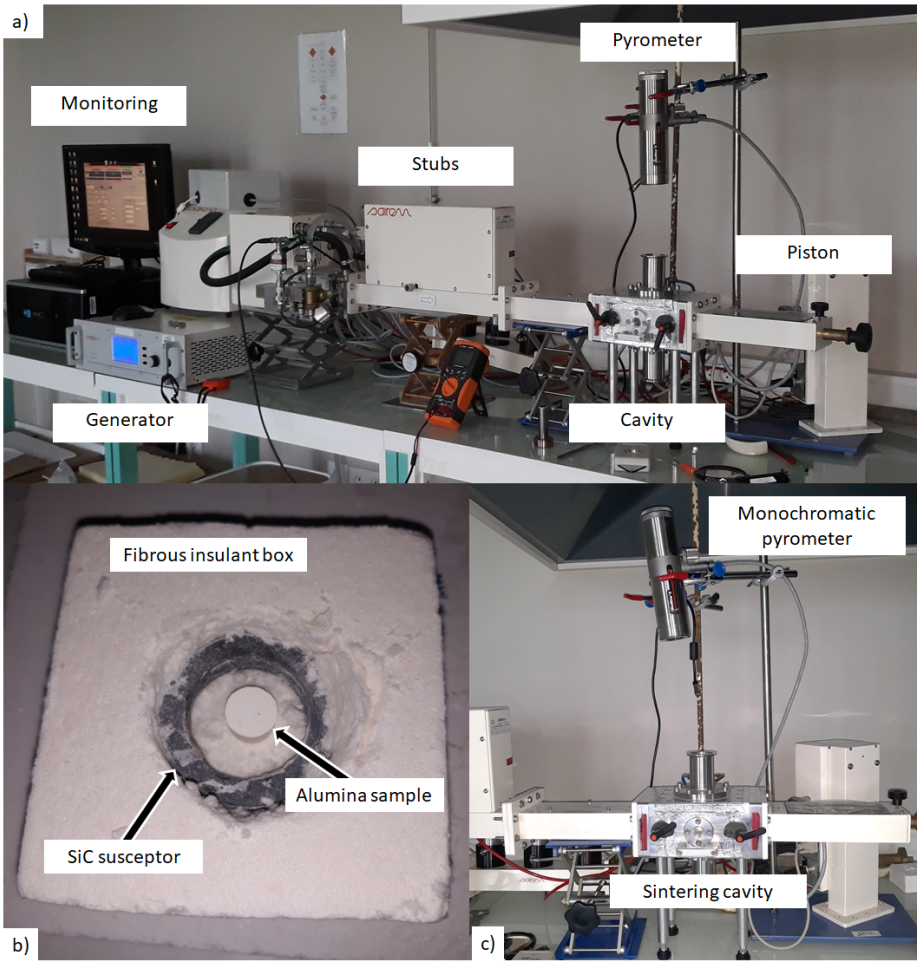

Figure 4: a) microwave sintering set-up, b) insulating box, c) microwave chamber

4.2. Comparison with conventional sintering law parameters

Thanks to the previous results, it could be considered that the modified SOVS model is correct for a conventional alumina sintering process with slow ramps. Then, simulations are performed for ramps corresponding to heating by

MW ($1.5°C/s$ and $2.5°C/s$) from room temperature to $1600°C$. The results are shown in Figure 5. The average gap between the simulations and experimental measurements are around 20%. So, the correlations used for conventional sintering in modified SOVS model does not allow to match to measured density in MW. The initialization of sintering seems to be shifted by about $100°C$, with a deviation that increases for the intermediate stage up to 15% at the end of sintering. Adaptations are necessary for the modified SOVS model described in the previous sections.

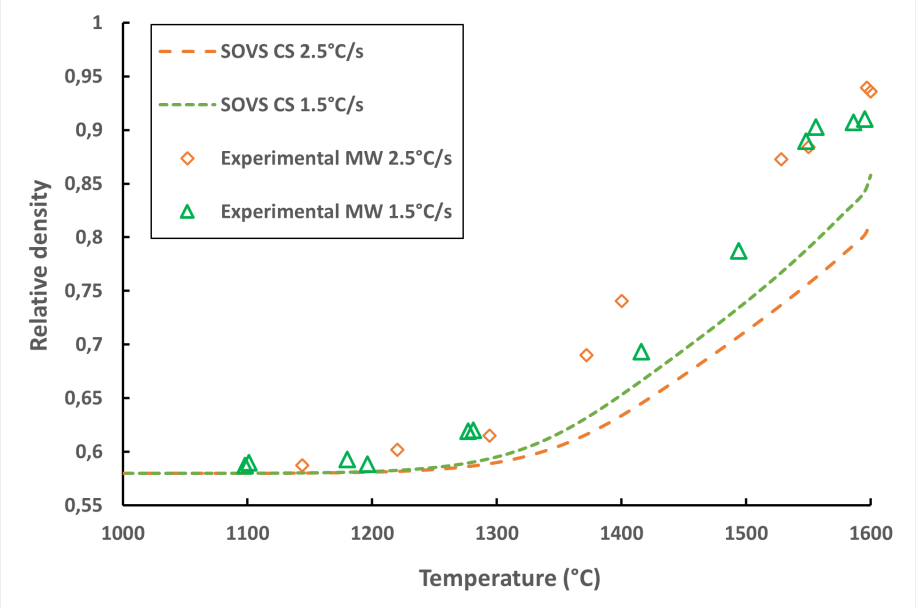

Figure 5: Simulation with modified SOVS model: comparison with MW sintering measurements

4.3. Identifications of microwave law parameters

The gap between the simulations and the experimental results can be explained by a possible microwave effect caused by the electromagnetic field within the cavity or other factors through modification of the sintering mechanisms.

Although the origin is unknown, modifications in the model are necessary. By looking at the behaviour equation 5, it is possible to modify either the viscous part or the part containing the sintering stress. It was decided to adopt a more macroscopic approach by focusing only on the viscous part. As Manière et al. [13], it was decided to modify only the viscous part. Nevertheless, as expressed in reference [1], enhanced electric field at grain boundaries could explain the differences observed in the sintering mechanisms for microwave sintering. The viscosity law, expressed by Shinagawa [24] and used in modified SOVS model, is thermal and grain size dependant law given by Eq 8. The approach used in this model allows a correct match between the experimental results and the simulations for conventional heating. Nevertheless, for microwave sintering, these constants do not allow to match experimental relative densities (cf. figure 5). It was decided to adjust the shear viscosity by adjusting C_1 and C_2, in order to obtain lower viscosity values according to the temperature. This means that alumina sample would be able to densify at lower temperatures. To adjust the viscosity law for microwave sintering of alumina, it was decided to optimize the constants C_1 et C_2 for the new law η_{MW}:

$$\eta_{MW} = C_{1_{MW}} T exp\left(\frac{C_{2_{MW}}}{T}\right) d^3 \tag{14}$$

Sensitivity studies are led to find the influences of constants. Decreasing C_1 leads to an increase of the slope of the resulting densification simulated curve and to small shift at the beginning of the curve. On the other hand, small increasing C_2 leads to shift densification curve to higher temperatures. Simulations are launched in order to optimize the constants from the experimental data. By trials and errors, the best combination for each ramps has been determined. The values of C_1 and C_2 constants are resumed in the Table 2.

	Conventional sintering[15]	Microwave sintering
$C_1(Pa.s.K^{-1}.m^{-3})$	7.82×10^{17}	2.50×10^{13}
$C_2(K)$	3.43×10^4	4.52×10^4

Table 2: Conventional and microwave constants values for viscosity correlation

Then, the viscosity correlation for microwave sintering is used to run new densities simulations with three temperature ramps. The curves comparing simulations to experimental relative density data are collected in Figure 6. The results show that the modifications of the viscosity law make possible to improve the microwave sintering model, since for both curves the average deviation is close to 1%. Then it is possible to conclude that modifications in microwave model allow to approximate the relative density of alumina sample according to the temperature.

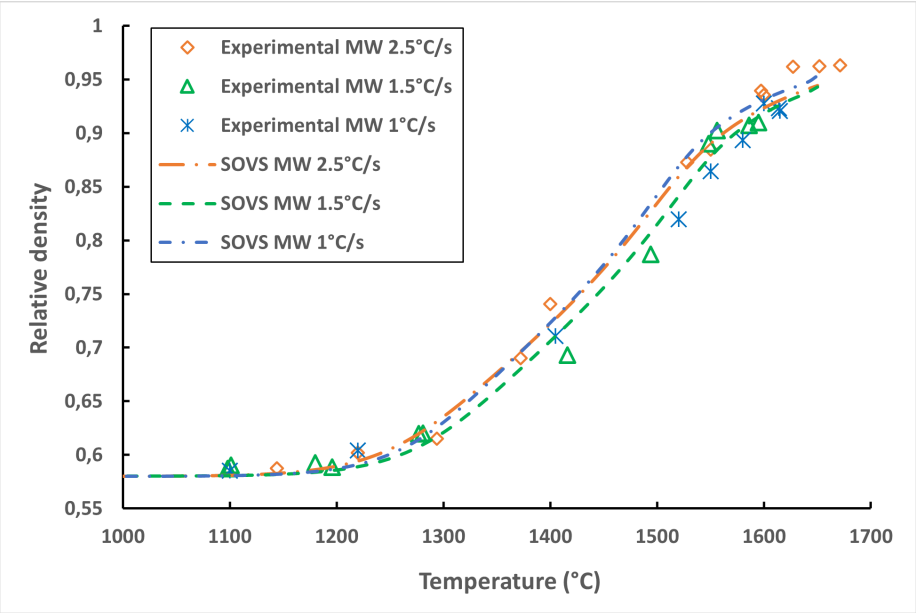

Figure 6: Comparison between experimental data and simulations with viscosity law modified for MW sintering

The robustness of the model is tested as a function of dwell time. In order to test the influence of dwell time and the influence of time, simulations and experiments are led from $1400°C$ and $1500°C$ according to $2.5°C/s$. Then, the temperature is hold, and the dwell times are included from 0 min to 30 min. Results, in Table 3, show that the relative differences between simulation and measurements are lower than 3%. So, it is possible to consider that the MW model is able to take into account both of thermal and time dependences.

Dwell temperature ($^{\circ}C$)	Dwell time (min)	Experimental final relative density	Simulation final relative density	Relative difference (%)
$1400^{\circ}C$	0 min	0.731 ± 0.01	0.722	2.49
$1400^{\circ}C$	2 min	0.863 ± 0.01	0.859	0.56
$1400^{\circ}C$	5 min	0.898 ± 0.01	0.909	-1.25
$1400^{\circ}C$	7 min	0.920 ± 0.01	0.923	-0.31
$1400^{\circ}C$	15 min	0.947 ± 0.01	0.946	0.11
$1400^{\circ}C$	30 min	0.966 ± 0.01	0.962	0.43
$1500^{\circ}C$	0 min	0.830 ± 0.01	0.834	0.58
$1500^{\circ}C$	2 min	0.930 ± 0.01	0.935	0.53
$1500^{\circ}C$	5 min	0.957 ± 0.01	0.956	-0.10
$1500^{\circ}C$	7 min	0.953 ± 0.01	0.963	1.00
$1500^{\circ}C$	15 min	0.965 ± 0.01	0.977	1.18
$1500^{\circ}C$	30 min	0.967 ± 0.01	0.987	2.10

Table 3: Comparison of simulations and experimental relative density measurements for microwave sintering with variable dwell time at $1400^{\circ}C$ and $1500^{\circ}C$ according to a ramp of $2.5^{\circ}C/s$

Previously validated ramps in microwave sintering are fast and produce very dense aluminas in less than 30 minutes. Nevertheless, it is legitimate to ask whether the model is also correct for slower ramps. Furthermore, at equivalent ramp rates, are there any differences with conventional sintering? For this purpose, interrupted sintering tests (without dwell time) are carried out with a ramp of $10^{\circ}C/min$ for both conventional and microwave sintering. The results are shown in the figure 7. It can be observed that microwave modelling works well with lower ramps, the average difference is around 3%. Moreover, compared to conventional sintering, there seems to be a microwave effect. At the same temperature, the density in microwave is around 20% higher than in conventional sintering. Of course, a bias regarding the temperature reading on

the pyrometer could interfere with our results.

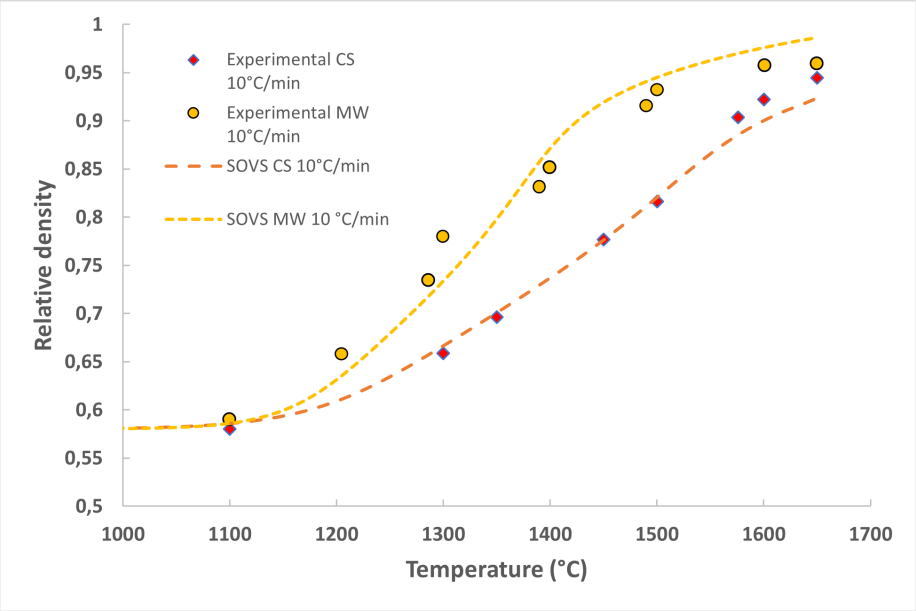

Figure 7: Comparison between experimental data and simulations with viscosity law modified for MW and CS sintering, equivalent ramp at $10°C/min$

4.4. Discussion

In the model, densification goes along with an increase in grain size. The viscosity is therefore modified throughout the sintering process. Intrinsically and macroscopically, viscosity must also be linked to the microwave field because this modifies the behaviour of charged species of the material at the molecular scale. In order to highlight this specific effect, Figure 8 compares the evolution of the calculated viscosity at constant grain size value ($\frac{\eta}{d^3}$) as a function of temperature for the two types of sintering.

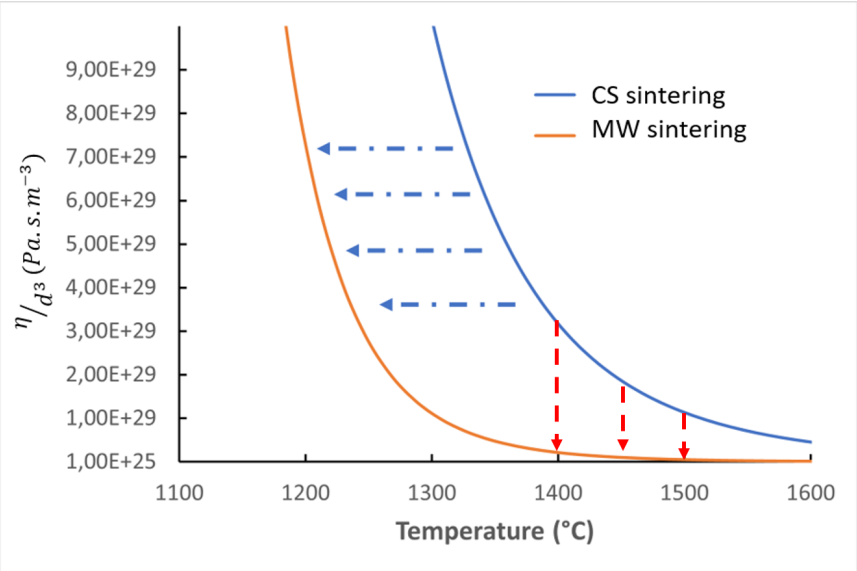

Figure 8: Comparison of the ratio shear viscosity by the grain diameter according to the temperature for CS and MW sintering

The modifications of C_1 and C_2 in microwave correlation corresponds to a modification of the material behaviour. It may be noticed that the calculated equivalent viscosity is systematically lower under microwave radiation than for conventional sintering. The new viscosity law is not simply modified in its form but moved to equivalent viscosities at lower temperatures of about $100°C$. It corresponds to the shift observed in the Figure 5, considering, as a first approach, that the temperature reading error of the pyrometer is not significant. This means that the densification seems to start at lower temperature in MW than in CS sintering. Fundamentally, shear viscosity can be linked to diffusion coefficients at grain boundaries. In Ref. [23], the constants C_1 and C_2 in viscosity law in Eq. 8 are linked to the shear to materials parameters as:

$$C_1 = \frac{1}{3}\frac{k}{47\Omega h D_0} \tag{15}$$

$$C_2 = \frac{Q_d}{k} \tag{16}$$

$$D_b = D_0 exp\left(-\frac{Q_d}{k}\right) \tag{17}$$

where Ω is the vacancy volume (in m^3), h the effective boundary width, D_b the boundary diffusion coefficient (in $m^2.s^{-1}$), D_0 the frequency factor (in $m^2.s^{-1}$), k Boltzmann constant ($\approx 1.3806 \times 10^{-23} J.K^{-1}$), T the temperature (in K), Q_d the equivalent of activation energy for boundary diffusion (in $kJ.mol^{-1}$). Supposing that Ω and h are constant, the ratio between the CS and MW shear equivalent viscosities could be expressed according to diffusion coefficient D_d as:

$$\frac{\eta_{MW}}{\eta_{CS}} \approx \frac{D_{0_{CS}} exp\left(\frac{-Q_{d_{CS}}}{kT}\right)}{D_{0,MW} exp\left(\frac{-Q_{d_{MW}}}{kT}\right)} \approx \frac{D_{b_{CS}}}{D_{b_{MW}}} \ll 1 \tag{18}$$

Figure 9 represents the evolution of calculated $\frac{\eta_{MW}}{\eta_{CS}}$ versus temperature. It could be noticed that the impact of electric field of the microwave is increased at high temperatures beyond $1500K$. This viscosity ratio in MW and in CS proves that coefficient diffusion is highly improved (from 10 to 50 times) in microwave sintering. Theses values means that microwave could modify mechanisms at grain boundaries and increases the values of diffusion coefficient and mobility of species. This approach could confirm hypotheses such as those of Rybakov [6, 8] concerning an increased mobility of charged species with the microwave.

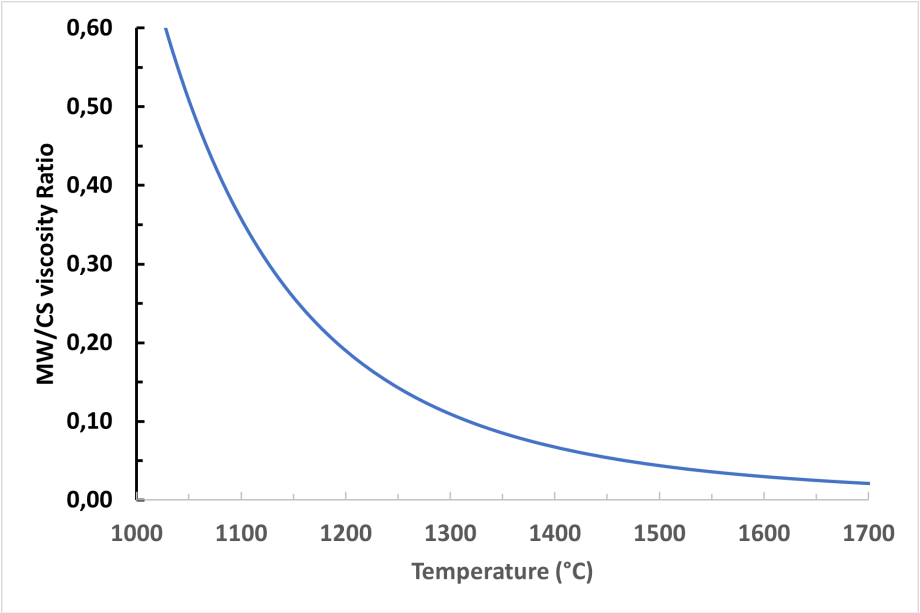

Figure 9: Shear viscosity ratio between MW and CS

5. Conclusion and outlook

In this study, the modified SOVS model is used on a doped submicronic alumina. The original model is slightly modified from experimental data. The grain growth law is modified and expressed as a function of density, regardless of temperature. This allows to take into account of MgO doping in this submicronic alumina. After the modifications, the simulations allow to validate the model for the conventional sintering.

Then, the conventional model is adapted from experimental results of the microwave sintering. A macroscopic approch has been followed and the viscosity law has been adapted. It appears that a modification of the viscosity law coefficients C_1 and C_2 allows to describe correctly the sintering behaviour as a function of time and temperature. Simulations are performed, and the new constants are determined by confronting to experimental measurements by tri-

als and errors. The new constants for microwave are $C_{1_{MW}} = 2.50 \times 10^{13}$ (versus $C_{1_{MW}} = 7.82 \times 10^{17}$ in CS [15]) and $C_{2_{MW}} = 4.52 \times 10^{4}$ (versus $C_{2_{MW}} = 3.23 \times 10^{4}$ in CS [15]), and correspond to lower values of apparent viscosity, leading on a faster densification. Then, the microwave model is compared with experimental measurements and validated according temperature and time. Moreover, sintering are performed in CS and MW with the same ramp ($10°C/min$), these tests seem to show that there is a microwave effect on alumina. The microwave radiation would have an impact on the mobility of charged species beyond a temperature of about 1500 K and could lead to obtaining an apparent viscosity 50 times lower. This results in faster sintering. In conclusion, this work shows that it is possible to adapt submicronic alumina conventional model to microwave sintering. This model takes into account the temperature, the time and leads to a correct prediction of the densification of the alumina in conventional and microwave sintering.

The described model is used for alumina, but by determining few parameters it may be possible to adapt it to another material. Moreover, due to the small size of the samples the temperature field is considered as homogeneous. With SEM observations, no density or grain size heterogeneity are observed. But the high heating ramp could generate heterogeneous thermal field which could lead to microstructural properties gradients in particular for bigger samples. It could be interesting to associate the mechanical model to a thermal model to take into account thermal gradient inside sample.

Thanks

The authors express their gratitude to the Communauté d'Agglomération Maubeuge Val de Sambre and to the Hauts-de-France Polytechnic University for the funding of the thesis work of Maxence Renaux.

References

[1] M. Oghbaei, O. Mirzaee, Microwave versus conventional sintering: A review of fundamentals, advantages and applications, Journal of Alloys and Compounds 494 (1-2) (2010) 175–189. doi:10.1016/j.jallcom.2010.01.068.

[2] F. Zuo, A. Badev, S. Saunier, D. Goeuriot, R. Heuguet, S. Marinel, Microwave versus conventional sintering: Estimate of the apparent activation energy for densification of alpha-alumina and zinc oxide, Journal of the European Ceramic Society 34 (12) (2014) 3103–3110. doi:10.1016/j.jeurceramsoc.2014.04.006.

[3] K. Orlik, Y. Lorgouilloux, P. Marchet, A. Thuault, F. Jean, M. Rguiti, C. Courtois, Influence of microwave sintering on electrical properties of BCTZ lead free piezoelectric ceramics, Journal of the European Ceramic Society 40 (4) (2020) 1212–1216. doi:10.1016/j.jeurceramsoc.2019.12.010.

[4] H. Curto, A. Thuault, F. Jean, M. Violier, V. Dupont, J.-C. Hornez, A. Leriche, Coupling additive manufacturing and microwave sintering: A fast processing route of alumina ceramics, Journal of the European Ceramic Society 40 (7) (2020) 2548–2554. doi:10.1016/j.jeurceramsoc.2019.11.009.

[5] K. H. Brosnan, G. L. Messing, D. K. Agrawal, Microwave sintering of alumina at 2.45 GHz, Journal of the American Ceramic Society 86 (8) (2003) 1307–1312.

[6] K. I. Rybakov, S. V. Egorov, A. G. Eremeev, V. V. Kholoptsev, I. V. Plotnikov, A. A. Sorokin, Ultra-rapid microwave sintering employing thermal instability and resonant absorption, Journal of Materials Research 34 (15) (2019) 2620–2634. doi:10.1557/jmr.2019.232.

[7] R. M. Young, R. McPherson, Temperature-Gradient-Driven Diffusion in

Rapid-Rate Sintering, Journal of the American Ceramic Society 72 (6) (1989) 1080–1081. doi:10.1111/j.1151-2916.1989.tb06278.x.

[8] K. Rybakov, E. Olevsky, E. Krikun, Microwave Sintering: Fundamentals and Modeling, Journal of the American Ceramic Society 96 (4) (2013) 1003–1020. doi:10.1111/jace.12278.

[9] F. Zuo, S. Saunier, S. Marinel, P. Chanin-Lambert, N. Peillon, D. Goeuriot, Investigation of the mechanism(s) controlling microwave sintering of alpha-alumina: Influence of the powder parameters on the grain growth, thermodynamics and densification kinetics, Journal of the European Ceramic Society 35 (3) (2015) 959–970. doi:10.1016/j.jeurceramsoc.2014.10.025.

[10] T. Frueh, I. Ozer, S. Poterala, H. Lee, E. Kupp, C. Compson, J. Atria, G. Messing, A critique of master sintering curve analysis, Journal of the European Ceramic Society 38 (4) (2018) 1030–1037. doi:10.1016/j.jeurceramsoc.2017.12.025.

[11] D. Bouvard, S. Charmond, C. P. Carry, Finite Element Modelling of Microwave Sintering, in: Advances in Sintering Science and Technology, John Wiley & Sons, Ltd, 2009, pp. 171–180. doi:10.1002/9780470599730.ch17.

[12] A. E. T. Elgendy, A.-H. Abdel-Aty, A. A. Youssef, M. A. A. Khder, K. Lotfy, S. Owyed, Exact solution of Arrhenius equation for non-isothermal kinetics at constant heating rate and n-th order of reaction, Journal of Mathematical Chemistry 58 (5) (2020) 922–938. doi:10.1007/s10910-019-01056-7.

[13] C. Manière, S. Chan, E. A. Olevsky, Microwave sintering of complex shapes: From multiphysics simulation to improvements of process scalability, Journal of the American Ceramic Society 102 (2) (2019) 611–620. doi:10.1111/jace.15892.

[14] E. A. Olevsky, D. Dudina, Field-Assisted Sintering: Science and Applications, Springer International Publishing, 2018. doi:10.1007/978-3-319-76032-2.

[15] C. Van Nguyen, S. Sistla, S. Van Kempen, N. Giang, A. Bezold, C. Broeckmann, F. Lange, A comparative study of different sintering models for Al_2O_3, Journal of the Ceramic Society of Japan 124 (4) (2016) 301–312. doi:10.2109/jcersj2.15257.

[16] H. Riedel, B. Blug, A Comprehensive Model for Solid State Sintering and Its Application to Silicon Carbide, in: Multiscale Deformation and Fracture in Materials and Structures, Vol. 84, Kluwer Academic Publishers, Dordrecht, 2002, pp. 49–70. doi:10.1007/0-306-46952-9_4.

[17] T. Kraft, H. Riedel, Numerical simulation of solid state sintering; model and application, Journal of the European Ceramic Society 24 (2) (2004) 345–361. doi:10.1016/S0955-2219(03)00222-X.

[18] V. V. Skorokhod, E. A. Olevskii, M. B. Shtern, Continuum theory of sintering. II. Effect of the rheological properties of the solid phase on the kinetics of sintering, Powder Metallurgy and Metal Ceramics 32 (2) (1993) 112–117. doi:10.1007/BF00560033.

[19] E. A. Olevsky, Theory of sintering: From discrete to continuum, Materials Science and Engineering: R: Reports 23 (2) (1998) 41–100. doi:10.1016/S0927-796X(98)00009-6.

[20] M. Abouaf, J. L. Chenot, G. Raisson, P. Bauduin, Finite element simulation of hot isostatic pressing of metal powders, International Journal for Numerical Methods in Engineering 25 (1) (1988) 191–212. doi:10.1002/nme.1620250116.

[21] N. Cox, Modeling shape distortion of 3-D printed aluminium oxide parts during sintering, Tech. rep., University of Pittsburgh (2018).

[22] M. W. Reiterer, K. G. Ewsuk, J. G. Arguello, An Arrhenius-Type Viscosity Function to Model Sintering Using the Skorohod-Olevsky Viscous Sintering Model Within a Finite-Element Code, Journal of the American Ceramic Society 89 (6) (2006) 1930–1935. doi:10.1111/j.1551-2916.2006.01041.x.

[23] K. Shinagawa, Micromechanical modelling of viscous sintering and a constitutive equation with sintering stress, Computational Materials Science 13 (4) (1999) 276–285. doi:10.1016/S0927-0256(98)00132-3.

[24] K. Shinagawa, Finite Element Simulation of Sintering process (Microscopic Modelling of Powder Compacts and Constitutive Equation for Sintering), JSME international journal. Ser. A, Mechanics and material engineering 39 (4) (1996) 565–572. doi:10.1299/jsmea1993.39.4_565.

[25] J. Croquesel, D. Bouvard, J.-M. Chaix, C. P. Carry, S. Saunier, S. Marinel, Direct microwave sintering of pure alumina in a single mode cavity: Grain size and phase transformation effects, Acta Materialia 116 (2016) 53–62. doi:10.1016/j.actamat.2016.06.027.

[26] M. I. Mendelson, Average Grain Size in Polycrystalline Ceramics, Journal of the American Ceramic Society 52 (8) (1969) 443–446. doi:10.1111/j.1151-2916.1969.tb11975.x.

[27] R. Morrell, Handbook of Properties of Technical and Engineering Ceramics. Part 1: An Introduction for the Engineer and Designer., H.M.S.O, 1985.